doi:10.1111/evo.12744

An integrated analysis of phenotypic selection on insect body size and development time

Daniel J. Eck,[1] Ruth G. Shaw,[2] Charles J. Geyer,[3] and Joel G. Kingsolver[4,5]

[1]*School of Statistics, University of Minnesota, 313 Ford Hall, 224 Church Street S.E., Minneapolis, Minnesota, 55455*

[2]*Department of Ecology, Evolution, and Behavior and Minnesota Center for Community Genetics, University of Minnesota, 100 Ecology Building, 1987 Upper Buford Circle, St. Paul, Minnesota, 55108*

[3]*School of Statistics, University of Minnesota, 313 Ford Hall, 224 Church Street S.E., Minneapolis, Minnesota, 55455*

[4]*Department of Biology, University of North Carolina, Chapel Hill, 27599*

[5]*E-mail: jgking@bio.unc.edu*

Received December 23, 2014
Accepted July 18, 2015

Most studies of phenotypic selection do not estimate selection or fitness surfaces for multiple components of fitness within a unified statistical framework. This makes it difficult or impossible to assess how selection operates on traits through variation in multiple components of fitness. We describe a new generation of aster models that can evaluate phenotypic selection by accounting for timing of life-history transitions and their effect on population growth rate, in addition to survival and reproductive output. We use this approach to estimate selection on body size and development time for a field population of the herbivorous insect, *Manduca sexta* (Lepidoptera: Sphingidae). Estimated fitness surfaces revealed strong and significant directional selection favoring both larger adult size (via effects on egg counts) and more rapid rates of early larval development (via effects on larval survival). Incorporating the timing of reproduction and its influence on population growth rate into the analysis resulted in larger values for size in early larval development at which fitness is maximized, and weaker selection on size in early larval development. These results illustrate how the interplay of different components of fitness can influence selection on size and development time. This integrated modeling framework can be readily applied to studies of phenotypic selection via multiple fitness components in other systems.

KEY WORDS: **Aster models, fitness components, life-history tradeoffs, *Manduca sexta*, natural selection.**

There is abundant evidence for phenotypic and genotypic selection on quantitative traits in natural populations (Kingsolver et al. 2001; Siepielski et al. 2009). Most estimates of the strength and pattern of phenotypic selection — more than 90% — are based on individual components of fitness, rather than metrics of lifetime fitness (Kingsolver and Diamond 2011). The resulting inferences may reflect the nature of phenotypic selection only weakly or not at all, to the extent that components of fitness differ in their relationships to traits. For studies that do evaluate lifetime fitness of individuals or genotypes, the distribution of fitness is generally not normal: it is typically highly skewed and often multimodal, with a large mode at zero, corresponding to individuals that die without reproducing. Thus, the assumption of normally distributed residuals required for the standard statistical analyses does not hold, making inference and hypothesis testing about selection problematic. Aster models were developed to address this challenge. This approach produces statistically valid models for fitness by taking into account the dependence of later expressed fitness components on those expressed earlier and also by employing appropriate probability models for each component (Geyer et al. 2007; Shaw et al. 2008). Aster models for inferring phenotypic selection have been validated by Shaw and Geyer (2010).

EVOLUTION
INTERNATIONAL JOURNAL OF ORGANIC EVOLUTION

In many species, including most insects, variation in age at first reproduction is a major component of fitness that can have a large effect on the population growth rate and similar metrics of fitness (Roff 2002). This information is typically difficult both to obtain and to incorporate into analyses of fitness. As a result, integrated analyses of phenotypic selection that consider variation in time to reproduction are currently limited to relatively few cases of long-term studies with birds, mammals, and plants (Childs et al. 2004; Ozgul et al. 2009; Clutton-Brock and Sheldon 2010; Ozgul et al. 2010; Charmantier and Gienapp 2014).

In this article, we extend previous aster models to incorporate age at reproduction in the model for fitness. These new models (R package `aster2`, Geyer 2015) allow us to specify "dependence groups" that represent different life-history stages, as well as variation in the age at which individuals reach these stages, and include these in the model for fitness.

Holometabolous insects have distinct larval, pupal, and adult (reproductive) life stages, and rates of growth and development within and across life stages have important effects on fitness. For example, Kingsolver et al. (2012) used common garden field studies with *Manduca sexta* (Lepidoptera: Sphingidae) to estimate phenotypic selection on body size and age at different developmental stages. However, that study estimated selection via survival, reproduction, and generation time separately, and therefore could not quantify how selection operates over the entire life cycle, nor identify the interplay of fitness components in their contributions to lifetime fitness. Here, we describe and apply `aster2` models to these data to gain an integrated view of phenotypic selection on size and age across development, along with insight into the interplay of fitness components, in this study system. We discuss the utility of these methods in clarifying selection in other systems.

All statistical analyses discussed in this article are carried out in full in the accompanying technical report (Eck et al. 2015) produced using the R function `knitr` so all results in them are actually produced by the code shown and hence are fully reproducible.

Methods

STUDY SYSTEM AND FIELD STUDIES

The Tobacco Hornworm, *M. sexta*, is found in Central America and the southern United States, with eastern populations extending north into New York and Massachusetts. In the southeastern United States, including North Carolina, cultivated tobacco and tomato are dominant host plants for *M. sexta*, which can be an important agricultural pest in these systems. Our field studies used tobacco cultivars (see below).

After hatching, *M. sexta* larvae grow and develop rapidly through five (occasionally more) larval instars, growing from $\sim$ 1 mg to $\sim$ 8–12 g in body mass in a few weeks under optimal conditions. Rates of larval growth and development are strongly influenced by environmental temperatures and host plant quality. Toward the end of the final instar, larvae stop feeding and wander off the host plant to pupate nearby in the soil. A facultative pupal diapause is determined by larval photoperiod, such that *M. sexta* populations have multiple generations per year in most areas (2–3 generations/year in North Carolina). Because pupae do not feed, maximum larval mass at wandering strongly determines pupal and adult size and the number of eggs (oocytes) produced by females.

For *M. sexta*, both host plant quality and larval susceptibility to natural enemies are important determinants of survival to adult reproduction. For example, in the southeastern United States including North Carolina, the larval parasitoid *Cotesia congregata* (Hymenoptera: Braconidae) is often a major source of larval mortality. Thus, rapid rates of early larval growth and development may strongly influence survival to reproduction in this system.

Here, we consider a field selection study of *M. sexta* conducted in a cultivated tobacco garden in the Mason Farm Biological Reserve, Chapel Hill NC, in July 2010. Details are fully described by Kingsolver et al. (2012); we briefly summarize here. Prior to the study, the garden plot (12 m by 20 m in size) was tilled and fertilized. Tobacco plants (*Nicotiana tabacum*, var. LA Burley 21) were grown from seeds in pots in the greenhouse at the University of North Carolina-Chapel Hill , and then they were transplanted to the field garden. A total of 60 plants in six rows were used in the study plot, with a single buffer row of tobacco plants around the perimeter of the study plot. The plants were allowed to establish for $\sim$ 4 weeks prior to the start of the study; plants that did not thrive after transplanting were replaced. The garden was watered daily, and insect herbivores were removed weekly by hand from each plant. To minimize larval predation by birds and social wasps, plants were covered with bridal veil netting just prior to the study. The netting excludes large predators but allows access to the caterpillars by parasitoids, including *C. congregata*.

To initiate the study, *M. sexta* eggs were collected from pesticide-free tobacco plants at the NC State Agricultural Extension Farm, Clayton NC, approximately 100 km from Chapel Hill. Eggs were allowed to hatch in the lab and were maintained individually on tobacco leaves in an environmental chamber at 25 °C. with a 16L:8D light cycle during the 1st and 2nd larval instars. Body mass and age at the start of the 2nd and 3rd instars were measured. Following molt into the 3rd instar, each larva was randomly assigned to a plant (four larvae per plant, to avoid larval competition for food) in the study plot. Each larva was marked using water-based nail polish on the tip of the dorsal horn (and reapplied after each molt). This allowed us to track individuals in the field throughout the study (Kingsolver et al. 2012).

During daily field censuses, we recorded the presence or absence of each larva. Recapture probabilities (given alive) for larvae consistently exceeded 90%. At the start of the 4th and 5th instar, the mass and age of each larva were recorded, and the larva was returned to its plant.

When larval mass late in the 5th instar exceeded 5 g (about 14–16 days), larvae were removed from the field and reared individually on tobacco leaves in petri dishes in an environmental chamber at 26.7 °C (16L:8D light cycle) until wandering. Mass and age at wandering were recorded, then each larva was placed in a wooden block (Yamamoto 1969) at 25 °C to pupate. Pupal mass was measured at 7 days after wandering to ensure the pupal cuticle hardened prior to handling. Pupae were placed in plastic cups with moistened soil, kept at 20 °C, and checked daily each morning until eclosion (considered as age of reproduction). Estimates of potential fecundity for adult females (48 h after eclosion) were obtained by dissecting out and counting the number of ovarioles at stage 6 or later (Yamauchi and Yoshitake 1984; Diamond and Kingsolver 2010a).

STATISTICAL ANALYSES

Our analyses evaluate the relationship between fitness and three traits, age (since hatching) at the second instar stage, mass at that age, and mass at eclosion. Individuals reproduce only if they survive to eclosion and they eclose only if they survive to pupation. Thus there is inherent dependence of each component of fitness on survival to that life-history stage. We here use an individual's ovariole count as the best proxy for its lifetime fitness. No measure of fitness is perfect, and this one has the limitation that the data do not span the complete life cycle, but they do span the great majority of it. Ovariole count will henceforth be referred to simply as observed fitness. The unconditional expectation of ovariole count for an individual at the beginning of the experiment will be referred to as expected fitness. To address the problem that lifetime fitness generally does not conform to any standard statistical distribution, in part because many individuals die without reproducing, aster directly models this distribution by explicitly modeling the distributions of its underlying components, as well as their dependence structure.

The underlying dependence structure of development for females in this dataset can be represented by an aster graph (Fig. 1). The first arrow indicates an individual's survival to pupation, where survival is modeled as a Bernoulli random variable, shown as P in the graph. For an individual that survived to pupation, we account for the timing of metamorphosis by using dependence groups in the graphical model. For example, the next three nodes in this graph (T_{33_0}, T_{33_1}, and T_{33_2}) together represent a three-way switch where a particular *M. sexta* can only transition into one of these three nodes. The T_{33_0} node is 1 if the individual died before reaching eclosion. For simplicity, all individuals that died following pupation and before eclosion are treated as dying at age 33 days, the day when the first individual in our study eclosed; this has no effect on the results. The T_{33_1} node is 1 if the individual remained as a pupa on day 33, and the T_{33_2} node is 1 if the individual eclosed at age 33. In general, if the predecessor is 0, then every component in the dependence group is 0. However, if the predecessor is 1 then exactly one component of the response in the dependence group is 1 and the rest are 0. The dependence groups at each successive age follow a similar pattern, albeit with only two nodes because all mortality after pupation but before reproduction is treated as occurring on day 33. No individual survived past day 40. The dependence groups are modeled as multinomial with the number of categories equal to the number of nodes in the dependence group. For any age i when an individual has eclosed, $T_{i_2} = 1$, the ovariole counts, labeled B_i, are modeled with a zero-truncated Poisson distribution, given that females reaching eclosion are expected to have more than zero ovarioles.

To estimate fitness, we modeled both females and males, recognizing that the graph corresponding to males does not have ovariole count nodes, otherwise the graphs are the same. In order to model the probability of an individual female's survival to pupation we included the information for the males in our statistical model, because an individual can be sexed only once it reaches the pupal stage.

We use an unconditional aster model (see Section 5 of the supporting technical report, Eck et al. 2015; for the meaning of terminology for aster models) to obtain comprehensive estimates of lifetime fitness by modeling these distinct fitness components jointly according to this graphical structure. Once the distributions of all the nodes in the aster model and their dependence structure are specified, phenotypic selection analysis proceeds by regressing the nodes considered to correspond to lifetime fitness, here female ovariole counts, on the phenotypic predictors of interest. This regression, conducted as an unconditional aster model, takes into account all life-history stages. In the unconditional aster model unconditional expected fitness is a monotone function of fitness on the canonical parameter scale, which is modeled as a linear or quadratic function of the traits (justified by the Appendix of Shaw and Geyer 2010; and our Appendix). To assess directional selection, as well as the curvature of the fitness function, we consider aster models having as predictors three traits: mass at second instar, mass at eclosion, and age at second instar. In the model selected by goodness of fit tests, fitness represented on the canonical parameter scale is a general quadratic function of the two mass traits and a linear function of age at second instar. We note that general quadratic functions include as predictors not only the square of each trait but also pairwise interactions between the traits (Blows and Brooks 2003; Shaw and Geyer 2010). As shown in Table 1, all terms in this model are statistically significant.

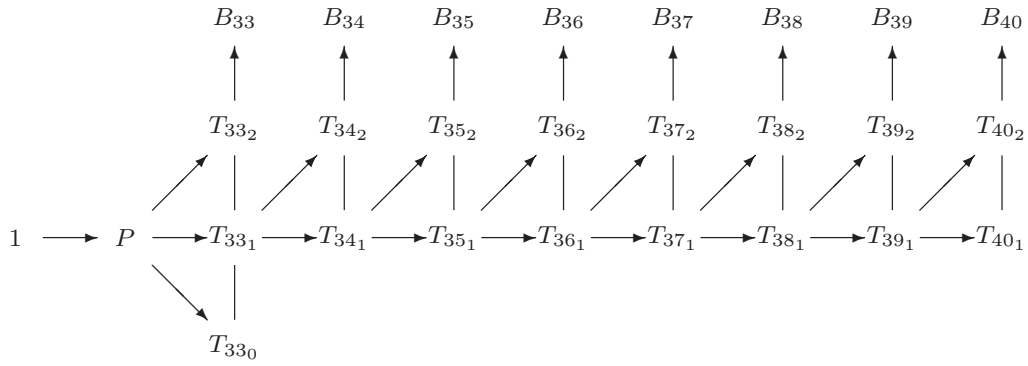

Figure 1. Aster graph for female *M. sexta*. Arrows go from predecessor nodes to successor nodes. Lines (that are not arrows) link dependence groups. Nodes are labeled by their associated variables. *P* node is pupation, *T* nodes are survival, and eclosion indicators, *B* nodes are ovariole counts. Subscripts indicate age (in days), subsubscripts indicate variables in the same dependence group (0 = death, 1 = surviving but preeclosion, 2 = eclosion at this time). For simplicity, all deaths after pupation but before reproduction were modeled as occurring on day 33. No individuals survived past day 40.

Table 1. Rao tests for smaller models. *P*-values and degrees of freedom for Rao tests of three smaller models against the larger model that includes linear, quadratic, and interaction term for the two mass traits and a linear term for age at second larval instar stage.

null model	df	*P*-value
removes quadratic terms for mass at second instar	2	3.37×10^{-8}
removes quadratic terms for mass at eclosion	2	$< 10^{-10}$
removes linear term for age at second instar	1	7.88×10^{-5}

In order to compare models of interest, a Rao test is used where the reference distribution is χ^2 with degrees of freedom equal to the difference of free parameters between the two models. Fitness landscapes (Lande and Arnold 1983; Shaw and Geyer 2010) are then generated from the model selected by the Rao test. This is done by evaluating expected fitness for hypothetical individuals having various values of the phenotypic traits (mass at second instar, mass at eclosion, and age at second instar) ranging over a grid and then making a contour plot of these values (Fig. 2).

The analyses described above account for variation in survival and ovariole counts but do not take into account that, in a growing population, earlier produced offspring contribute more to fitness than those produced later. To address this aspect of fitness, we extended the aster models described by Shaw and Geyer (2010). The population growth rate parameter (λ) for the observed population of *M. sexta* is estimated from the stable age equation (Fisher 1930), which is equation (A4) in the Appendix, as the basis of accounting for individuals' age at reproduction in their lifetime fitness.

We examine the effects of λ on fitness by fitting different models determined by equations (A1) and (A3) in the Appendix. All these models make expected fitness a monotone function of "fitness on the canonical parameter scale" that has the same functional form (quadratic in both mass at 2nd instar and mass at eclosion and linear in age at 2nd instar). They differ in what they consider expected fitness. The first kind of model, those described up to this point, considers fitness to be number of offspring. The second kind of model, which we are now introducing, considers fitness to be number of offspring weighted to account for population growth rate (λ), offspring at age t getting weight $e^{-\lambda t}$ by (A3) in the Appendix. If the population is growing, then offspring get more weight if produced earlier and less weight if produced later. Because these weights are dimensionless quantities, these models estimate relative fitness (fitness divided by mean fitness), whereas models of the first kind estimate absolute fitness (in units of number of offspring).

Results

Larval mortality prior to pupation was 23%, including 2% mortality due to parasitism by *C. congregata*. Field studies suggest that rates of larval mortality vary seasonally in this region (Diamond and Kingsolver 2010b; Kingsolver et al. 2012).

The phenotypic selection analysis detected relationships between lifetime fitness and all three traits considered as predictors. The aster model that includes the linear and quadratic terms for the two mass traits and their interaction, as well as the linear term for age at second larval instar stage, was chosen based on the Rao test. This model is chosen over the model that is full quadratic (including interactions) in all three traits ($P = 0.105$, Rao test, 3 degrees of freedom). All Rao tests that considered immediately smaller models were rejected, see Table 1.

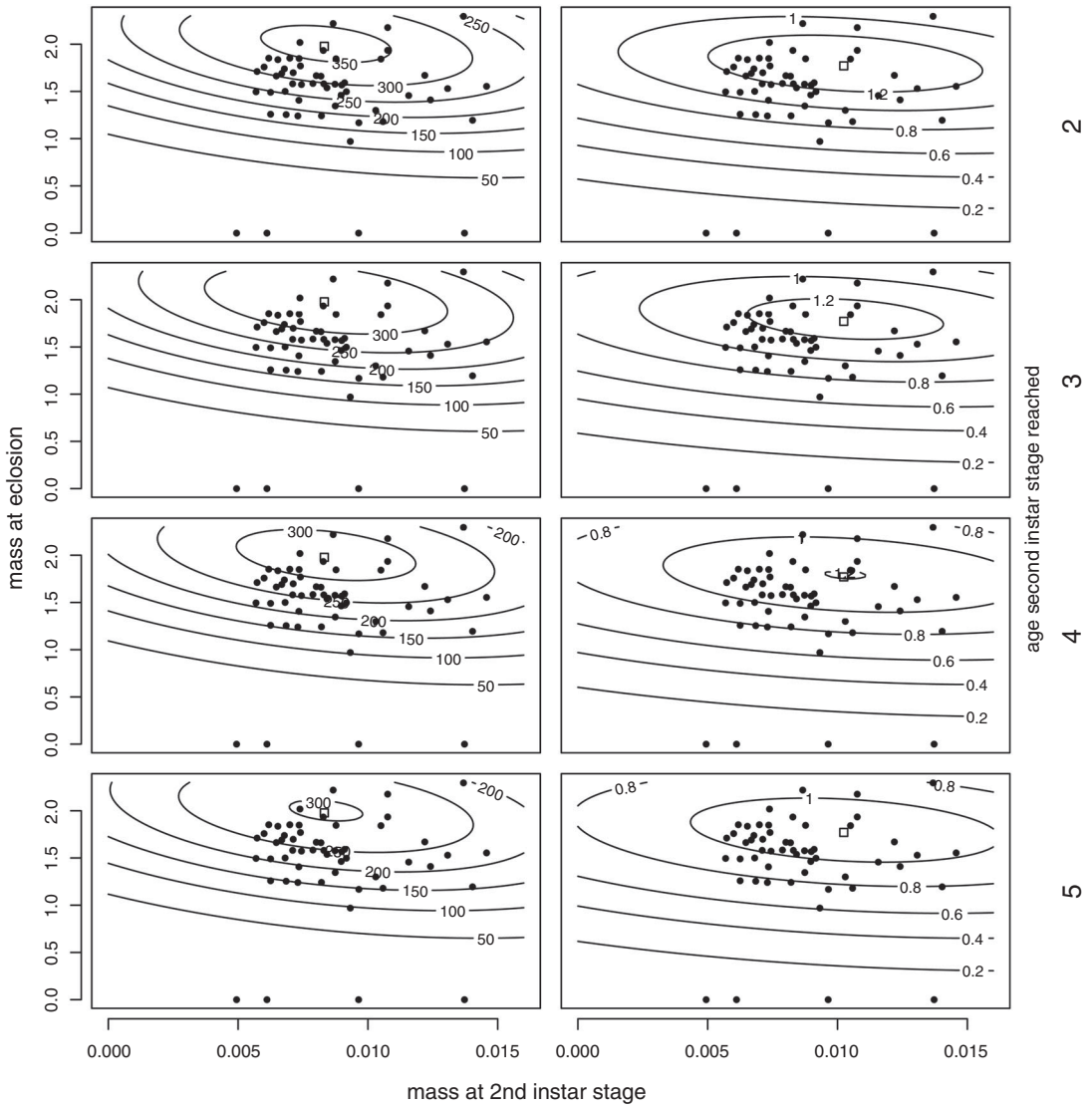

Figure 2. **Fitness landscapes without (left column) and with (right column) adjustment for population growth rate λ. Numbers on contours are absolute fitness (unconditional expected ovariole counts) in the left column and are relative fitness (absolute fitness divided by its average over the population) in the right column. All plots display fitness as contours versus mass at eclosion and mass at 2nd instar stage. Boxes denote locations of maxima. Maximum values are, from top to bottom, (left column) 363.6, 342.4, 322.4, 303.6 (right column) 1.39, 1.28, 1.20, and 1.14.**

The fitness landscape generated from this model shows that absolute fitness not adjusted for population growth rate (unconditional expected ovariole count, left column of Fig. 2) is predominantly explained by an individual's mass at eclosion. As mass at eclosion increases, unconditional expected ovariole count increases with a maximum found for female *M. sexta* weighing roughly 2 grams at eclosion, beyond which fitness declines. Considering mass at the second instar stage, the estimated contours viewed in relation to the observed data suggest that selection is largely directional with fitness inversely related to this trait, despite significant curvature of the fitness function in relation to this trait. In addition, unconditional expected ovariole count declines with increasing age to 2nd instar (left column of Fig. 2). For example, the maximum unconditional expected ovariole counts decline by 16% as age to 2nd instar increases from 2 to 5 days. This effect is largely due to the effects of age at 2nd instar on survival to eclosion: slower development (later age at 2nd instar) is associated with lower survival.

Absolute fitness (unconditional expected ovariole count) predicted from the model for individuals that survive to eclosion

range from 102.7 to 301.37. But observed ovariole counts for these individuals are larger ranging from 173.8 to 350.3. The reason for the discrepancy is that the former take survival into account and the latter do not (they ignore individuals that did not survive to eclosion).

The preceding analysis accounts for survival and ovariole count as components of fitness, but does not account for the role of variation in timing of reproduction in fitness variation. To incorporate this effect we consider population growth rate.

From the estimates of unconditional expected ovariole count at each age produced by the aster model we obtain via the stable age equation (A4) the estimate $\hat{\lambda} = 0.122$. The large positive value of λ indicates a rapidly growing population. Such large estimates of population growth rate are typical of experiments that do not have all sources of natural mortality and all sources of failure to reproduce, (c. f., Shaw et al. 2008; Example 1 reanalyzing data of Lenski and Service 1982).

The relative fitness landscape taking into account population growth and timing of reproduction (right column of Fig. 2) is qualitatively different from the landscape not so adjusted (left column of Fig. 2). When population growth rate is taken into account, maximum fitness occurs at a lower mass at eclosion and at a higher mass at the second instar larval stage. In Fig. 2 we can see that directional selection on mass at the second instar stage is weaker when the population growth rate is taken into account. This suggests that, in this study, variation in generation time does contribute importantly to patterns of phenotypic selection on the two mass traits.

Discussion

Variation in timing of reproduction is an important component of fitness variation in many organisms, and traits that influence it may undergo strong phenotypic selection. As a result, rates of development and other traits that affect age of first reproduction or reproductive schedules can importantly influence overall fitness. Our aster models provide an integrated statistical framework for estimating selection on traits via their effects on survival, ovariole counts and timing of reproduction.

The selection analyses of *M. sexta* in our study population identify two key traits: mass at eclosion, and age at 2nd instar. We detected stabilizing selection on mass at eclosion with the optimum near to the top of the observed range of values for this trait, but still within the range, such that fitness declines at still greater values. Reaching 2nd instar at earlier ages is associated with greater fitness (Fig. 2). However, these traits contribute to fitness via different components: mass at eclosion via fecundity, earlier age at 2nd instar through survival and timing of reproduction. More rapid development rates (reaching second instar at earlier ages) may allow larvae to escape key parasitoids and other natural enemies and increase survival (Diamond and Kingsolver 2010b; Kingsolver et al. 2012). For these data, variation in survival and ovariole counts appears to be more important than variation in timing of reproduction in determining selection on these traits (Fig. 2). Fitness was more subtly (though significantly) related to mass at 2nd instar; though rate of early larval development is under substantial directional selection, mass at this early stage is selected more weakly, largely in the direction of lower values.

Life-history tradeoffs among survival, fecundity, and generation time are common in many organisms (Roff 2002). Similarly, phenotypic and genetic correlations between traits can lead to opposing selection on the traits via different fitness components. The analyses presented here allow us to estimate phenotypic selection and fitness landscapes that integrate all three of these fitness components. A key result of these analyses is that incorporating generation time into fitness alters the pattern and strength of selection on larval and adult mass in *M. sexta*. In particular when population growth rate is taken into account, the strength of directional selection on mass at the 2nd instar decreases, and maximum fitness occurs at a higher mass at the 2nd instar but at a lower mass at eclosion (Fig. 2). These changes occur in part because age at 2nd instar is strongly positively correlated with age at eclosion and first reproduction, but is negatively correlated with mass at 2nd instar (Kingsolver et al. 2012). These effects could not be detected in previous analyses that considered selection on each fitness component separately (Kingsolver et al. 2012).

The aster analyses presented here account for development rate by using the multinomial distribution to model transitions through stages; they thus illustrate a new capability of aster modeling. This capability enables statistical modeling of selection via variation in the timing of life-history events through the discounting of later produced offspring in a growing population, in addition to any direct association of development rate with absolute reproductive output. As theory shows (Fisher 1930) and our analyses suggest, this discounting can play an important role in modulating individual fitness. In many temperate and tropical regions, variation in age of first reproduction and the number of generations per year is widespread in many insect populations (Roff 2002). It will be of interest to learn from future empirical studies of phenotypic selection how discounting of age-specific reproduction influences fitness surfaces more generally.

ACKNOWLEDGMENTS

We thank Sarah Diamond and two anonymous reviewers for comments on previous versions of the manuscript. Research supported in part by NSF IOS-1120500 to J.G.K.

DATA ARCHIEVING

The data of this paper is available at University of Minnesota digital conservancy http://dx.doi.org/10.13020/D6F59K.

LITERATURE CITED

Blows, M. W., and R. Brooks. 2003. Measuring nonlinear selection. Am. Nat. 162:815–820.

Charlesworth, B. 1980. *Evolution in age-structured populations*. Cambridge Univ. Press, Cambridge, UK.

Charmantier, A., and P. Gienapp. 2014. Climate change and timing of avian breeding and migration: evolutionary versus plastic changes. Evol. Appl. 7: 15–28.

Childs, D. Z., M. Rees, K. E. Rose, P. J. Grubb, and S. P. Ellner. 2004. Evolution of size-dependent flowering in a variable environment: construction and analysis of a stochastic integral projection model. *Proc. R. Soc. Lond. B* 271:425434

Clutton-Brock, T., and B. C. Sheldon. 2010. Individuals and populations: the role of long-term, individual-based studies of animals in ecology and evolutionary biology. *Trends Ecol. Evol.* 25: 562–573.

Diamond, S. E., and J. G. Kingsolver. 2010a. Environmental dependence of thermal reaction norms: host plant quality can reverse the temperature-size rule. *Am. Nat.* 175:1–10.

——,. 2010b. Fitness consequences of host plant choice: a field experiment. Oikos 119:542–550.

Eck, D. J., R. G. Shaw, C. J. Geyer, and J. G. Kingsolver. 2015. Supporting data analysis for "An integrated analysis of phenotypic selection on insect body size and development time." Technical Report No. 698, revised, School of Statistics, University of Minnesota. http://hdl.handle.net/11299/172272.

Fisher, R. A. 1930. *The genetical theory of natural selection*. Clarendon Press, Oxford, UK.

Geyer, C. J. 2015. R package aster2 (aster models), version 0.2-1. http://cran.r-project.org/package=aster2.

Geyer, C. J., S. Wagenius, and R. G. Shaw. 2007. Aster models for life history analysis. *Biometrika* 94:415–426.

Kingsolver, J. G., and S. E. Diamond. 2011. Phenotypic selection in natural populations: what limits directional selection? *Am. Nat.* 177:346–357.

Kingsolver, J. G., S. E. Diamond, S. A. Seiter, and J. K. Higgins. 2012. Direct and indirect phenotypic selection on developmental trajectories in *Manduca sexta*. *Funct. Ecol.* 26:598–607.

Kingsolver, J. G., H. E. Hoekstra, J. M. Hoekstra, D. Berrigan, S. N. Vignieri, C. E. Hill, A. Hoang, P. Gilbert, and P. Beerli. 2001. The strength of phenotypic selection in natural populations. *Am. Nat.* 157:245–261.

Lande, R., and S. Arnold. 1983. The measurement of selection on correlated characters. *Evolution* 37:1210–1226.

Lenski, R. E., and P. M. Service. 1982. The statistical analysis of population growth rates calculated from schedules of survivorship and fecundity. *Ecology* 63:655662.

Ozgul, A., D. Z. Childs, M. K. Oli, K. B. Armitage, D. T. Blumstein, L. E. Olson, S. Tuljapurkar, and T. Coulson. 2010. Coupled dynamics of body mass and population growth in response to environmental change. *Nature* 466:482–485.

Ozgul, A., S. Tuljapurkar, T. G. Benton, J. M. Pemberton, T. H. Clutton-Brock, and T. Coulson. 2009. The dynamics of phenotypic change and the shrinking sheep of St. Kilda. *Science* 325:464-467.

Roff, D. A. 2002. *Life history evolution*. Sinauer Associates, Sunderland, MA.

Shaw, R. G., and C. J. Geyer. 2010. Inferring fitness landscapes. *Evolution* 64:2510–2520.

Shaw, R. G., C. J. Geyer, S. Wagenius, H. Hangelbroek, and J. R. Etterson. 2008. Unifying life-history analyses for inference of fitness and population growth. *Am. Nat.* 172:E35–E47.

Siepielski, A. M., J. D. DiBattista, and S. M. Carlson. 2009. It's about time: the temporal dynamics of phenotypic selection in the wild. *Ecol. Lett.* 12:1261–1276.

Yamamoto, R. T. 1969. Mass rearing of the tobacco hornworm. II. Larval rearing and pupation. *J. Econ. Entomol.* 62:1427–1437.

Yamauchi, H., and N. Yoshitake. 1984. Developmental stages of ovarian follicles of the silkworm, *Bombyx mori* L. *J. Morphol.* 179:21–31.

Associate Editor: W. Blanckenhorn
Handling Editor: J. Conner

Appendix: Adjusting Fitness for Population Growth Rate

The Appendix of Shaw and Geyer (2010) explains the multivariate monotone relationship between unconditional canonical parameters φ_j and unconditional mean value parameters μ_j in an aster model. The latter are the quantities of scientific interest, unconditional expectations of components of the response vector. The former are the ones specified by model formulas for many statistical reasons (Geyer et al. 2007). Now we must extend equations (A2) and (A3) of Shaw and Geyer (2010) to allow for population growth rate.

We replace (A2) by

$$\varphi_j(\mathbf{x}, \mathbf{z}) = a_j(\mathbf{x}) + w_j q(\mathbf{z}), \qquad j \in J. \tag{A1}$$

Here, J is the set of nodes of the full aster graph; j runs over individuals and nodes within individuals. The full-aster graph has one subgraph for each individual in the data. In our data, each subgraph looks like Figure 1 for a female or like Figure 1 with the ovariole count nodes omitted for a male. In (A1) $\mathbf{z}$ is the vector of phenotypic trait variables for an actual or hypothetical individual, $\mathbf{x}$ is a vector of other covariate variables, $\varphi_j(\mathbf{x}, \mathbf{z})$ is the canonical parameter value for node j. We have no other such variables $\mathbf{x}$ in our data, but the equations being rewritten from Shaw and Geyer (2010) allowed for them, so we keep them. This equation says that $\varphi_j(\mathbf{x}, \mathbf{z})$ is modeled as an arbitrary function of $\mathbf{x}$, which may vary from node to node, plus an arbitrary function of $\mathbf{z}$, which varies from node to node in only a very restricted way, the same function $q(\mathbf{z})$ being multiplied by node-specific weights w_j that do not depend on $\mathbf{z}$.

It then follows by the same argument that goes from (A2) to (A3) in Shaw and Geyer (2010) that (A1) implies

$$q(\mathbf{z}_1) > q(\mathbf{z}_2) \quad \text{if and only if} \quad \sum_{j \in J} w_j \mu_j(\mathbf{x}, \mathbf{z}_1) > \sum_{j \in J} w_j \mu_j(\mathbf{x}, \mathbf{z}_2). \tag{A2}$$

This argument holds for arbitrary real number weights w_j and arbitrary functions $q(\mathbf{z})$. We can think of $q(\mathbf{z})$ as the fitness landscape on the canonical parameter scale and of $\sum_{j \in J} w_j \mu_j(\mathbf{x}, \mathbf{z})$, considered as a function of $\mathbf{z}$ holding $\mathbf{x}$ fixed, as the fitness landscape on the mean value parameter scale.

In all previously published aster analyses, the weights w_j were zero or one so fitness on the mean value parameter scale is just the sum of terms with $w_j = 1$. This allows fitness to be the sum over only those nodes of the graph that contribute directly to fitness. In our data, these are the ovariole count nodes. (Other nodes contribute only indirectly through their effect on unconditional mean ovariole count.) For our data our first aster analyses were also of this form. But after population growth rate λ had been determined we refit the data using weights

$$w_j = f_j e^{-\lambda t_j} \tag{A3}$$

where f_j are the zero or one weights indicating nodes that contribute directly to fitness and t_j is the age of the individual at node j. This weighting accounts for population growth rate (Charlesworth 1980; p. 134).

In our data, there are no "other" (nonphenotypic) covariates $\mathbf{x}$, so $a_j(\mathbf{x})$ in (A1) becomes a_j and $\varphi_j(\mathbf{x}, \mathbf{z})$ and $\mu_j(\mathbf{x}, \mathbf{z})$ in (A1) and (A2) become $\varphi_j(\mathbf{z})$ and $\mu_j(\mathbf{z})$.

To estimate λ, we use the stable age equation (Fisher 1930; p. 26). In our context, this is

$$1 = \frac{1}{n} \sum_{j \in J} \mu_j(\mathbf{z}_j) f_j e^{-\lambda t_j} \tag{A4}$$

where n is the number of individuals in the data, $\mu_j(\mathbf{z}_j)$ is the mean value for node j with the phenotypic data for that individual plugged in, and the rest is as above.

In most applications of the stable age equation, starting with Fisher, the term $\mu_j(\mathbf{z}_j)$ in (A4) is written as the product of probability of survival to age t_j and the conditional expectation of number of offspring at age t_j given survival to age t_j. We use the notation in (A4) because $\mu_j(\mathbf{z}_j)$ is calculated directly by the aster software. Most applications of the stable age equation, starting with Fisher, do not average over all individuals in the data, as we do here. That is because those treatments do not allow for variation among individuals. Consequently, they use the same model for all individuals and apply the stable age equation to one individual (and hence to all because all are the same according to the model).

Having estimated λ and refit the aster model so fitness is adjusted for λ, we then take the fitness landscape adjusted for λ to be

$$w(\mathbf{z}) = \sum_{j \in K} \mu_j(\mathbf{z}) f_j e^{-\lambda t_j}, \tag{A5}$$

where on the right-hand side everything is as in (A4) except that now the summation runs over the set K of nodes for a single hypothetical female individual having phenotypic trait vector $\mathbf{z}$ (Charlesworth 1980; p. 134).

Comparison of (A4) and (A5) shows that if we replace $\mathbf{z}$ for this hypothetical individual by the covariate vector values $\mathbf{z}_j$ for actual individuals and average over all individuals in the data, we get 1. Thus (A5) is *relative fitness* (fitness divided by mean fitness). Call (A5) expected relative fitness adjusted for population growth rate.